Biophysical Chemistry 15 (1982) 157–167
Elsevier Biomedical Press



# ELECTRIC PROPERTIES AND STRUCTURE OF DNA RESTRICTION FRAGMENTS FROM MEASUREMENTS OF THE ELECTRIC DICHROISM

Stephan DIEKMANN [a,*], Wolfgang HILLEN [b], Manfred JUNG [a], Robert D. WELLS [c] and Dietmar PÖRSCHKE [a]

[a] *Max-Planck-Institut für Biophysikalische Chemie, Postfach 968, 3400 Göttingen, F.R.G.,* [b] *Technische Hochschule Darmstadt, Institut für Organische Chemie, Petersenstr. 22, 6100 Darmstadt, F.R.G., and* [c] *University of Wisconsin, Department of Biochemistry, Madison, WI 53706, U.S.A.*

Received 3rd September 1981

*Key words: DNA; Polarizability; Electric dichroism; Polyelectrolyte; Orientation mechanism*

The electric dichroism of 17 homogeneous DNA fragments, ranging in size from 43 to 4362 base-pairs, has been analyzed in high electric fields. The orientation of the small fragments can be described in terms of an induced dipole moment, whereas the large fragments are oriented according to a constant dipole mechanism. In the intermediate size range, DNA orients according to an induced dipole mechanism at low field strengths and according to a constant dipole mechanism at high field strengths. From these observations we propose an orientation mechanism with a saturating induced dipole. The induced dipole observed at low field strengths is saturated at a field strength $E_0$ within a transition range $E_m$ to give a constant dipole moment at high field strengths. These parameters together with the polarizability and the limit reduced dichroism are evaluated by a least-squares analysis of the experimental data. $E_0$ and $E_m$ are found to decrease with increasing chain length from $E_0 \approx 40$ kV/cm ($E_m \approx 14$ kV/cm) at 65 base-pairs to 10 kV/cm (6 kV/cm) at 194 base-pairs. The polarizability is found to increase with the square of the chain length, whereas the saturated dipole increases with chain length $N$ at low $N$ and goes to a limit value at high $N$. The temperature dependence of the orientation parameters is found to be very small. The values obtained for the limit dichroism are between $-1.0$ and $-1.3$ for chain lengths between 60 and 1000 base-pairs, whereas values around $-1.4$ are observed at chain lengths greater than 1000 base-pairs. These data indicate that electric fields extend the contour of DNA strands at high chain lengths from a weakly bent to a more linear form. The variations of the limit dichroism observed for short fragments suggest sequence-dependent differences in the secondary structure of the helix. The experimental results are compared with numerical calculations based on simple polyelectrolyte models. For short fragments the magnitude of several electrochemical parameters can be adequately explained by a polarization of the ion cloud around the DNA molecules. However, these polyelectrolyte models do not adequately describe the observed chain length dependence of the orientation phenomena.

## 1. Introduction

Electro-optical methods have already been used as tools for the analysis of macromolecular structures for a long time [1,2]. The main advantage of these methods is their high sensitivity, which allows the analysis of macromolecules in very dilute solutions. In the case of DNA, the electrodichroism can be measured easily and with high accuracy at concentrations as low as 10 $\mu$M. The strong orientation of DNA by electric fields is usually attributed to a polarization of the ion atmosphere around the polyelectrolyte [1,2]. The resulting dipole leads to a partial orientation of the molecules with their long axis parallel to the electric field. Due to the periodic arrangement of the bases the orientation of DNA can be easily followed by optical anisotropy measurements. Such measurements are expected to provide detailed information about the structure of the nucleic acid and the properties of its ion cloud. However, the

* Present address: Biochemical Laboratories, Harvard University, 7 Divinity Avenue, Cambridge, MA 02138, U.S.A.

0301-4622/82/0000–0000/$02.75 © 1982 Elsevier Biomedical Press

conclusions may be strongly affected by the orientation mechanism used to interpret the data. Until recently, interpretation of experimental data and selection of an appropriate mechanism were rendered particularly difficult by the heterogeneity of the available nucleic acid samples. Use of homogeneous restriction fragments avoids this problem. We have measured the electrodichroism of 17 restriction fragments over a wide range of field strengths. The experimental data have been analyzed in terms of various orientation mechanisms described in the literature. None of these mechanisms provided a satisfactory representation of our data. For this reason we propose a new orientation mechanism with a 'saturating induced dipole moment', which is a combination of the conventional induced dipole and constant dipole mechanism. The new mechanism provides an accurate representation of the experimental data for all DNA fragments investigated over a wide range of field strengths. Parameters obtained according to this model are compared with some numerical calculations on simple polyelectrolyte models.

## 2. Materials and methods

### 2.1. Preparation of samples

Most of the DNA fragments were prepared by known procedures from the recombinant plasmid pRW574 [3]. Since this plasmid contains a quadruple insert originating from the lactose genetic control region of *Escherichia coli*, some of the fragments contain the known binding sites for the respective regulatory proteins [4,5]. The 43-, 69-, 84-, 180-, 245-, 258-, 436- and 880-base-pair fragments result from digestion of the vector pVH51 [6] with the restriction endonuclease *Hae*III. The four fragments with a similar size around 430 base-pairs from this digest [4] coeluted from the RPC-5 column and are designated 430-pool. From this mixture the 436-base pair fragment was purified by RPC-5 chromatography on a small scale [7]. The 258-base-pair fragment was digested with *Hpa*II and the mixture of fragments was separated on RPC-5 [3] resulting in the purification of a 134- and a 64-base-pair piece. The 64-base-pair DNA from the lactose control region is designated $64_a$, and the respective DNA from the *Hpa*I digest of the 258-base-pair fragment is named $64_n$. The size and GC content of these fragments are derived from the known sequence [8–11] of of pVH51 [4]. The 1450-base-pair fragment was purified by RPC-5 chromatography from an *Eco*RI digest of pRT29 [12]. The vector pBR322 was used to examine the behaviour of a large DNA fragment. It is 4362 base-pairs in length and was linearized by a *Bam*HI digestion [13]. The 118-, 194- and 603-base-pair fragments were purchased from Bethesda Research Laboratories Inc., MD, U.S.A. (they result from an *Hae*III digest of $\phi$X174).

Prior to each measurement, approx. 0.5 absorbance units (260 nm) of the respective fragment in 1 ml solution were dialyzed against 0.7 l of 2 M NaCl and 0.1 mM EDTA once and then at least three times against 0.8 l of 1 mM NaCl + 1 mM sodium cacodylate + 0.2 mM EDTA.

The absence of any degradative activity in the samples was confirmed by gel electrophoresis on 5% acrylamide gels before and after the measurements.

Measurements were performed in the buffer system 1 mM sodium cacodylate, 1 mM NaCl, 0.2 mM EDTA, pH 7.1. The pH was adjusted by addition of HCl.

### 2.2. Field jump measurement

Field jump measurements were performed with an apparatus constructed by Grunhagen [14] with modifications of the optical detection system introduced by Porschke [15]. The reaction volume in the field jump cell was about 0.7 ml, the optical path length 0.97 cm, and the distance between the electrodes 0.63 cm. The resistance of the solutions at 20°C was 3.3 kΩ and the temperature jump in the cell, induced by the electrical field pulse at the highest field strengths, was 2°C at most.

Transmission changes due to electrical fields were recorded at 0, 54.8 and 90° orientation of the light vector (248.2 nm) with respect to the field vector. The transmission at the magic angle 54.8° was measured as a control for conformation changes induced by the electrical field. We found

no evidence for such conformation changes under the conditions of our experiments. The quotient of the absorbance changes at 0 and 90° was used as a further control. The theoretical value of 2 was measured in all cases within a few percent deviation. The reduced dichroism was obtained according to

$$\Delta\epsilon/\epsilon=(\Delta A_0-\Delta A_{90})/A \quad (1)$$

where $A$ is the isotropic absorbance determined on a Cary 219 spectrophotometer before the measurement and $\Delta A$ the absorbance change measured at 0 and 90° according to the subscript.

The absorbance at 260 nm was about 0.15 (23 $\mu$M nucleotides) for all solutions. At least 15 dichroism points were measured between 8 and 70 kV/cm for each sample (except the 4362-base-pair fragment: here between 8 and 50 kV/cm only 8 points are measured).

### 2.3. *Fitting procedure*

The experimental data were fitted by a procedure based on the simplex method of Nelder and Mead [16]. The basic idea of the simplex method is to construct a sequence of simplices which contract to the final estimates of the parameters fitting the measured data. In a three-dimensional parameter-space a simplex is defined by four distinct sets of parameters which represent the vertices of the simplex. The iteration process is terminated as soon as the variance of the sum FQS of the absolute errors evaluated at the vertices of the simplex falls below a preset value. This method is slightly modified and used to minimize FQS. Since the limit electric dichroism at infinitely high field strength $(\Delta\epsilon/\epsilon)_\infty$ enters linearly in the fitted equation (cf. section 4), the value of $(\Delta\epsilon/\epsilon)_\infty$ which minimizes the sum of absolute errors for a given set of the non-linear parameters ($E_0$, $E_m$ and $p$; cf. section 4) can be determined by solving a linear equation. Thus, it is sufficient to minimize FQS in a reduced, three-dimensional space spanned only by the non-linear parameters ($E_0$, $E_m$ and $p$). All calculations were performed using the facilities of the Gesellschaft für Wissenschaftliche Datenverarbeitung, Göttingen.

## 3. Comparison of various orientation mechanisms with experimental results

According to the symmetry of the double helical structure, DNA molecules should not exhibit a permanent dipole moment. However, various authors have demonstrated that DNA molecules orient in high electric fields according to a permanent dipole mechanism [17–19]. This contradiction has been discussed by several authors.

For example, Emonds-Alt et al. [18] have attributed such behaviour to the heterogeneity of DNA samples used for the measurements. According to these authors the orientation of individual DNA molecules follows an induced dipole mechanism, but the superposition of orientation curves for DNA molecules of different length results in experimental data suggesting the existence of a permanent dipole. This interpretation can be easily tested by using restriction fragments of uniform length and sequence. As shown in fig. 1, the electrodichroism measured for a 258-base-pair fragment can be represented with high accuracy by a permanent dipole mechanism but not by the induced dipole mechanism. Similar data are obtained for other fragments. Thus, the permanent dipole observed for DNA is not merely an artifact resulting from heterogeneous samples, although heterogeneity may have an influence on orientation data.

While the experimental data clearly suggest the existence of a permanent dipole, it remains obvious that the DNA should not have any appreciable 'intrinsic' permanent dipole. For this reason it has been suggested that an induced dipole moment is saturated at relatively low field strengths. Sokerov and Weill [19] have proposed such a mechanism following a suggestion of Shirai (unpublished data). According to these authors, integration over the orientation angles should be carried out over only half the space, since the electrostatic energy for the two symmetrical orientations $\theta$ and $\pi-\theta$ is equal. As for the permanent dipole mechanism, the interaction energy of the molecule with the field is linear with the field strength and the cosine of the orientation angle.

Another model was proposed by Hogan et al. [20]. As the primary cause of DNA orientation in

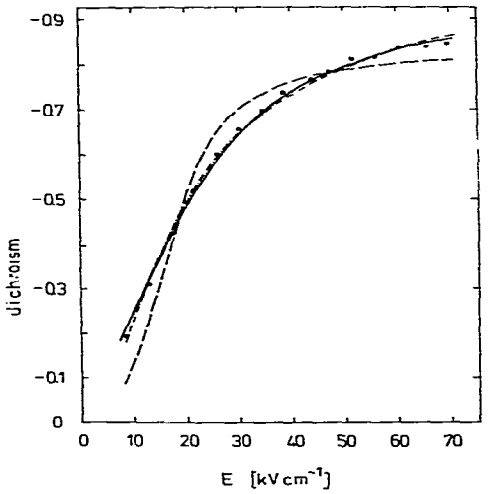


Fig. 1. Reduced dichroism of a 258-base-pair fragment as a function of the field strength. Experimental points with least-squares fit according to the permanent dipole (— · —), induced dipole (— — —) and the saturating induced dipole mechanism (————).

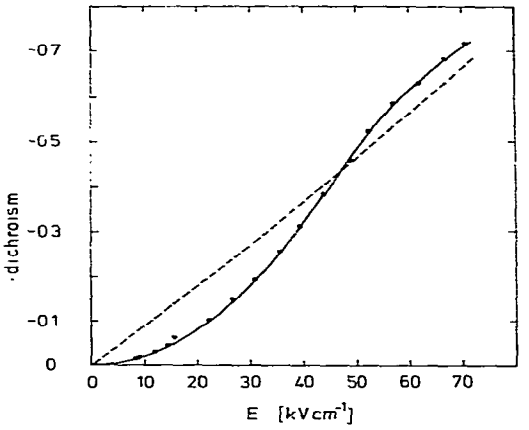


Fig. 2. Reduced dichroism of a 43-base-pair fragment as a function of the field strength. Experimental points (●) with least-squares fits according to the anisotropic ion flow (— — —) and induced dipole mechanism (————). The results of the saturating induced dipole mechanism are identical to those of the induced dipole mechanism in the whole field range.

an electric field, they propose the torque exerted on the polyion by an ion atmosphere that has lost cylindrical symmetry because of steady-state counterion flow: the centres of negative (DNA) and positive (counterions) charges no longer superimpose. This 'anisotropic ion flow' model predicts an orientation function which is equal to that for a saturated induced dipole.

We have found that the model of Sokerov and Weill [19] as well as that of Hogan et al. [20] adquately describes our data for chain lengths above 200 base-pairs. At chain lengths below 200 base-pairs, clear deviations are observed and for our shortest fragment (43 base-pairs) the shape of the experimental orientation curve is completely different from that expected according to the formalisms described above. However, the data obtained for the short fragment can be described with high accuracy by an induced dipole mechanism up to field strengths of 70 kV/cm (cf. fig. 2). These observations are in agreement with birefringence measurements of sonicated DNA [21]. At low field strengths the birefringence data can be represented by the induced dipole mechanism. Our results directly demonstrate that there is a transition from one domain, which can be described by an induced dipole mechanism, to another which can be described by a constant dipole mechanism. The transition depends upon both the chain length and the field strength.

## 4. The saturating induced dipole moment

Since none of the orientation mechanisms described in the literature [19,20] adequately describes our experimental data, we propose a new, extended mechanism. As discussed in section 3, the orientation proceeds according to an induced dipole mechanism at low field strength. The interaction is described by the energy term

$$U = -pE \cdot E/(2k_bT) \qquad (2)$$

where $p$ is the polarizability, $E$ the field strength and $k_bT$ the thermal energy. With increasing field strength the factor $pE$ goes to a limit at the field strength $E_0$; the limit value $pE_0$ corresponds to the saturated induced dipole. A comparison of this

formalism with experimental data indicates that the transition between the two mechanisms does not proceed abruptly but requires a transition range $E_m$. The transition function is defined according to

$$\theta = 1/(1+\exp((E-E_0)/E_m)) \quad (3)$$

This function varies between 1 at low field strength and 0 at high field strength and is designed to describe the transition between the induced dipole and the constant dipole mechanism. The formalism of the transition function corresponds to a field-induced transition controlled by a free energy. The free energy should contain a term which is linear in the field strength. The energy term for the 'saturating induced dipole' mechanism reads

$$U = -pE[E\theta + E_0(1-\theta)]/(2k_bT) \quad (4)$$

According to the standard procedure for the calculation of the orientation function [22] we arrive at the following expression for the reduced dichroism

$$\Delta\epsilon/\epsilon = \left\{\tfrac{4}{3}\left[\left\{e^u/\left(u^{1/2}\int_0^{u^{1/2}} e^{x^2}\,dx\right)\right\} - 1/u\right] - \tfrac{1}{2}\right\} \times (\Delta\epsilon/\epsilon)_\infty \quad (5)$$

where $(\Delta\epsilon/\epsilon)_\infty$ is the limit electric dichroism. Eq. 5 is solved by numerical procedures. At field strengths below the transition range the field dependence is exactly as described by a simple induced dipole mechanism. At high field strengths above the transition range the mathematics of the orientation function is not equivalent to that obtained for a permanent dipole mechanism.

The expression for the reduced dichroism contains four parameters which can be fitted to experimental data. We have used the fitting procedure described in section 2.3 and observed clearly defined error minima for all parameters. The accuracy of our experimental data and the quality of their representation by the saturating induced dipole mechanism are shown in figs. 1–3. These data also illustrate the limits of the other orientation mechanisms. The 43-base-pair fragment orients over the whole field range according to the induced dipole mechanism. Fig. 2 shows that for this short DNA fragment an induced dipole and the saturating induced dipole mechanism describe the data

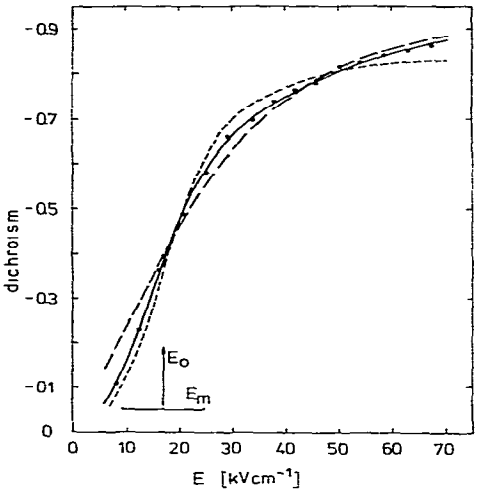


Fig. 3. Reduced dichroism of a 118-base-pair fragment as a function of the field strength. Experimental points with least-squares fits according to the anisotropic ion flow (— — —), the induced dipole (------) and the saturating induced dipole mechanism (————).

with high accuracy, whereas the anisotropic ion flow mechanism does not.

For a longer DNA fragment of 258 base-pairs, the induced dipole moment is already saturated at the lowest measured field strength (8 kV/cm, cf. fig. 1). Both the anisotropic ion flow and the saturating induced dipole mechanism describe the curve equally well, whereas the induced dipole mechanism does not. In the intermediate size range (118 base-pairs, fig. 3), experimental points can only be represented by the saturating induced dipole mechanism.

The parameters obtained according to the saturating induced dipole mechanism are compiled in table 1 for our DNA fragments. Some of these parameters are checked by independent procedures. For example, in the case of long DNA fragments with low $E_0$ values, the experimental data were fitted according to the constant dipole mechanism with only two fit parameters. The values for the limit dichroism and the dipole moment obtained from these fits were in close agreement with those obtained by the saturating induced

Table 1

Results of the dichroism at 20°C

| DNA base-pairs | %GC | Ends (restriction enzyme) | $(\Delta\epsilon/\epsilon)_\infty$ | $E_0$ (kV cm$^{-1}$) | $p$ (cm$^2$ V$^{-1}$) ($\times 10^{-35}$) | $E_m$ (kV cm$^{-1}$) | $m_s$ (C m) ($\times 10^{-30}$) |
|---|---|---|---|---|---|---|---|
| 43 | 49 | blunt | $-0.96\pm0.05$ | $\gtrsim 70$ | $105\pm10$ | – | – |
| $64_a$ | 55 | blunt | $-1.25\pm0.02$ | $41\pm2$ | $202\pm5$ | $13.5\pm1$ | $8280\pm400$ |
| $64_n$ | 59 | *Taq*I | $-1.29\pm0.02$ | $37.5\pm2$ | $219\pm5$ | $14\pm1$ | $8210\pm400$ |
| 69 | 52 | blunt | $-1.27\pm0.03$ | $35.5\pm1$ | $223\pm5$ | $10.8\pm0.5$ | $7910\pm400$ |
| 76 | 62 | blunt | $-1.11\pm0.03$ | $33.2\pm3$ | $269\pm5$ | $10.2\pm2$ | $8930\pm1000$ |
| 84 | 60 | blunt | $-1.21\pm0.02$ | $30.0\pm1$ | $335\pm5$ | $10.6\pm1$ | $10050\pm500$ |
| 95 | 46 | blunt | $-1.21\pm0.02$ | $24.0\pm1$ | $450\pm6$ | $9.0\pm1$ | $10800\pm600$ |
| 118 | 50 | blunt | $-1.04\pm0.02$ | $17.0\pm1$ | $690\pm8$ | $8.0\pm1$ | $11730\pm850$ |
| 134 | 47 | '5bl/3'*Taq*I | $-1.19\pm0.03$ | $14.3\pm1$ | $885\pm10$ | $8.0\pm2$ | $12660\pm1100$ |
| $180\pm3$ | $\approx 56$ | blunt | $-1.10\pm0.02$ | $11.0\pm2$ | $1120\pm30$ | $8.0\pm2$ | $12320\pm1500$ |
| 194 | 51 | blunt | $-1.08\pm0.02$ | $9.9\pm1$ | $1400\pm30$ | $6.0\pm1$ | $13860\pm1660$ |
| $245\pm4$ | – | '5bl/3'*Eco*RI | $-1.08\pm0.02$ | $<7$ | (4600) | $<4$ | $13800\pm200$ |
| 258 | 55 | blunt | $-1.17\pm0.02$ | $<7$ | (4790) | $<4$ | $15100\pm300$ |
| 430 pool | – | blunt | $-1.23\pm0.02$ | – | – | – | $14200\pm300$ |
| 436 | 57 | blunt | $-1.15\pm0.02$ | – | – | – | $13650\pm300$ |
| 603 | 43 | blunt | $-1.01\pm0.02$ | – | – | – | $15070\pm300$ |
| $880\pm13$ | $\approx 51$ | blunt | $-1.25\pm0.02$ | – | – | – | $12700\pm300$ |
| $1450\pm50$ | – | *Eco*RI | $-1.45\pm0.02$ | – | – | – | $12300\pm200$ |
| 4362 | 54 | *Bam*HI | $-1.38\pm0.04$ | – | – | – | $11000\pm2000$ |
| 95 [a] | 46 | blunt | $-1.18\pm0.02$ | $26.6\pm1$ | $443\pm6$ | $12.6\pm1$ | $11800\pm600$ |
| 95 [b] | 46 | blunt | $-1.21\pm0.02$ | $23.6\pm1$ | $428\pm6$ | $10.0\pm1$ | $10100\pm600$ |

[a] At 1.5°C.
[b] At 40°C.

dipole mechanism. In a similar way, data obtained for the shortest fragment (43 base-pairs) were fitted according to the induced dipole mechanism. As expected, the resulting limit dichroism and the polarizability were consistent with the value obtained by the saturating induced dipole mechanism.

According to our model, the dipole moment of a DNA fragment should be constant at field strengths above the saturation value. This was checked by a series of fits with the subsequent omission of more and more experimental points at field strengths well above the saturation field strength. If the dipole moment changes in this range of field strengths, the resulting fit parameters should show a clear trend. Instead, the values for all parameters show only small non-regular variations around the values found from the analysis using the maximum number of data points.

The temperature dependence of the parameters was analyzed by measurements at 2, 20 and 40°C with the 95-base-pair fragment. None of the parameters shows a significant temperature dependence. This result is in agreement with the counterion polarization model. Eq. 6 (cf. section 5), for instance, indicates that the polarizability is a function of $1/T$. The temperature dependence determined from the experimental data is slightly smaller, but still consistent with the theory within the limits of experimental accuracy.

## 5. Model calculations

Application of an external electrical field induces a current, perturbing the counterion distribution of the polyelectrolyte solution and removing the system from equilibrium. The analysis of

the resulting steady state is quite complex. Since the molecules are oriented by the field, not only the electrostatics of the steady state have to be calculated, but also hydrodynamic properties must be taken into account. Due to the lack of a complete theory, model calculations have been performed based on the assumption of a local equilibrium in the steady state. From these model calculations we expect to learn about the general behaviour of rod-like polyelectrolyte molecules in electrical fields.

Mandel [23] proposed a model of polyelectrolytes in which the macromolecule is represented by a cylinder with $N$ charged sites distributed regularly over its length. It is assumed that counterions cannot leave the region of the ion cloud around the polyion, either in a radial or in a longitudinal direction. The distribution of these mobile charges on the long axis of the macromolecule can then be calculated in the presence of a constant electrical field.

For small fields the dipole moment $m$ is given by

$$m = -nZ^2e_0^2b^2N^2E/12k_bT \quad (6)$$

where $Ze_0$ is the charge of the counterion, $b$ the distance between the fixed charges on the polyion, $k_bT$ the thermal energy, $E$ the field strength, and $n$ the number of counterions associated with the polyion. Hence, for small fields $m$ is linear in $E$ and depends roughly on the third power of the length of the macromolecule. With increasing field strength $m$ levels off and reaches a final saturated value $m_s$ at very high field strengths. In eq. 6 the proportionality factor with respect to $E$ represents the polarizability $p$ of the polyelectrolyte ion in the longitudinal direction due to the mobile charges. $p$ is given by

$$p = nZ^2e_0^2b^2N^2/12k_bT$$

The number of counterions $n$ can be replaced by

$$n = \alpha N = (1-2\phi)N$$

with $\alpha$ being the degree of dissociation of the polyion and $\phi$ the osmotic coefficient.

In these equations we use the parameters describing the charge spacing of DNA; only the degree of dissociation $\alpha$ (or the osmotic coefficient) is not known precisely. By varying $\alpha$, the polarizability $p$ can be brought into agreement with experimental values. This is done for a DNA molecule of 50 base-pairs yielding $\alpha = 0.075$. This value is too small by a factor of 10, reflecting the fact that in Mandel's theory the counterion repulsion is not taken into account [24]. All other quantities which can be compared with our experimental values (dipole moment $m_s$; saturation field strength $E_0$ and field range $E_m$ determined graphically from the transition between the range where the dipole moment $m$ is a linear function of the field strength and the range with constant dipole $m = m_s$) turn out to be too large by factors of 3–8. For these parameters the low field approximation is no longer valid. Thus, the saturation transition and the saturated dipole moment $m_s$ have been calculated with the complete Mandel theory. The disagreement of these quantities with the experimental values disappears by assuming that the probability of counterions binding to a specific binding site is limited to a maximal value. If this maximum is chosen to be two counterions per phosphate of the DNA, all calculated quantities are in agreement with the experimental data for the shortest DNA fragment. However, with increasing lengths of DNA, deviations between theoretical and experimental values become large.

On the basis of Mandel's model (without corrections for counterion repulsion), Neumann and Katchalsky [25] obtained an approximate equation for the dipole moment of DNA. Substituting again the DNA charge spacing parameters, the dipole moment $m_s$ and the polarizability are not changed and the saturation field strength $E_0$ and field range $E_m$ are slightly smaller as predicted by Mandel's model. However, $E_0$, $E_m$ and $m_s$ are still not in quantitative agreement with the experimental values.

Another calculation procedure based on the same physical model is proposed by McTague and Gibbs [26]. The partition function of the system is determined by recursion relations introducing a correction due to nearest-neighbour counterion interaction. This model does not even qualitatively describe our measurements at low fields. At high fields, the dipole moment continues to grow with

the field, in contrast to experimental results. Introduction of this kind of counterion repulsion into Mandel's model also fails to describe our experimental data especially at low fields. Therefore, we conclude that the counterion repulsion correction used by McTague and Gibbs leads to incorrect results.

Oosawa [27] calculated the mean square electric moment due to thermal fluctuations of the bound counterions taking into account the excess free energy resulting from a non-uniform distribution of counterions. This free energy incorporates a counterion repulsion energy. Using this theory, Hornick and Weill [28] and later Neumann and Katchalsky [25] proposed a correction term to the formulas, eqs. 6 and 7, for the dipole moment and the polarizability, respectively. Instead of a required counterion repulsion potential these authors calculate the polarizability using the unscreened cylindrical potential of the DNA. This approach predicts a concentration dependence of the polarizability which is not observed experimentally (unpublished results).

Manning [29] calculated the contribution of the condensed counterions to the low field polarizability implicitly taking into account counterion repulsion. This result is equal to Mandel's polarizability term (eq. 7) divided by a repulsion term which for DNA reads

$$F=[1-2(|z|\xi-1)\ln(\kappa_s b)]$$

where $\kappa_s$ is the Debye-Hückel screening parameter, $\xi$ the charge density parameter, $b$ the linear separation of the DNA charges (1.7 Å for DNA), and $Z$ the counterion charge.

When reasonable values [29] are substituted for each parameter, the calculated polarizability is too small by a factor of 2–3 for the shortest measured fragments, but becomes equal to the experimental value at about 120 base-pairs (see fig. 4). For longer fragments an increasing deviation between theory and experiments is obtained. Furthermore, Manning's theory does not determine the saturation behaviour and is thus restricted to low fields. Finally, Manning's model predicts that the polarizability should increase with ionic strength in disagreement with experimental data (unpublished results).

All the microscopic theories discussed above predict a dependence of the low field polarizability on the third power of the length of the molecules. However, this behaviour is not observed experimentally. Instead, we find a second power dependence (see fig. 4) which goes through the origin. Thus, for DNA molecules shorter than 43 base-pairs, no deviation from this second power dependence is expected. These microscopic theories can be compared with macroscopic models treating the DNA as a rotational ellipsoid with freely movable charges on the surface in a non-conducting medium [28,30]. These simple models yield polarizabilities which are of the same order of magnitude as the experimental results. The length dependence is smaller than the third power and thus closer to the qualitative experimental length dependence than the microscopic theories. A preliminary study of Fixman [31] also yields a length dependence of the polarizability smaller than the third power. The polarizabilities calculated with this theory are smaller that the measured values.

The saturated induced dipole moments $m_s$ show a strong increase with chain length for small fragments (fig. 5), but reach a plateau value for fragments with more than 200 base-pairs. These experimental data are not consistent with Mandel's

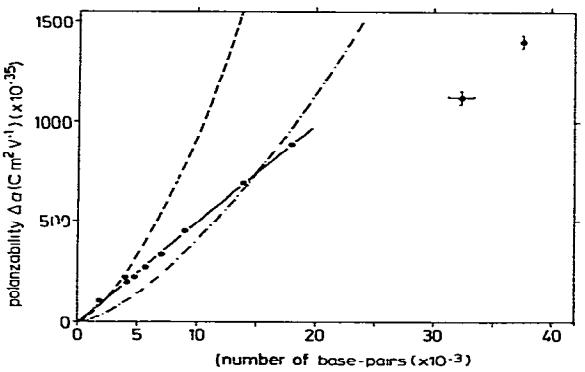


Fig. 4. Polarizability versus the second power of the number of base-pairs, (●) experimental points with error bars (up to the fragment with 134 base-pairs the errors are too small to be shown), (------) theoretical behaviour of the Mandel model ($\alpha=0.075$), (·–·–·) Manning's model. The solid line connects the experimental points indicating that the polarizability increases with the square of the length up to about 140 base-pairs.

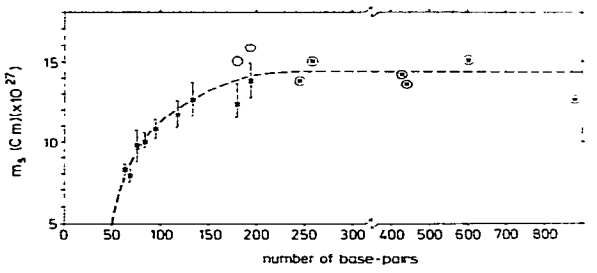


Fig. 5. Saturated induced dipole moment $m_s$ versus number of base-pairs, (x) experimental points with errors (for fragments with more than 200 base-pairs the errors are too small to be shown). (O) values obtained by a fit with the saturated induced dipole moment mechanism (two-parameter fit). For fragments with more than 200 base-pairs both values coincide.

theory, which predicts an increase in $m_s$ with the square of the chain length. The limit value of $m_s$ observed at relatively low chain lengths has not been predicted by any of the published theories. From the analysis of orientation time constants, we found a persistence length of about 500 Å for the conditions of our experiments [32]. Thus, the dipole moment $m_s$ levels off at chain lengths which approximately correspond to the persistence length. This result suggests that helix pieces of persistence length might be 'units', which are polarized by the electric field. However, it is important for the interpretation of this result to notice that the orientation relaxation times of the fragments with more than 200 base-pairs still increase with increasing number of base-pairs. Thus, the overall dimension of helices clearly increases with the number of base-pairs in this range of chain lengths. Apparently, the concept of charge separation over the entire length of the molecule is not suitable for the longer molecules.

The anisotropic ion flow model of Hogan et al. [20] also assumes a strong charge separation. As a consequence, their model predicts the value of $A$ to increase also with the square of the molecular length. However, for the longer fragments ($> 200$ base-pairs) investigated this behaviour is not observed.

## 6. Discussion

A major difficulty in the analysis of electro-optical data is the selection of an appropriate orientation mechanism. We have used an orientation mechanism based upon a particularly extensive set of data. These data suggest a transition from a regime with an induced dipole to another one with a saturated dipole. When this transition is accounted for, the resulting orientation mechanism provides a satisfactory explanation for a number of observations which have been unrelated up to now. Our mechanism is a logical extension of the orientation mechanisms used previously. Not only does this mechanism accurately describe our data but also the various parameters obtained by our mechanism are reasonable and consistent. For example, the existence of a transition in the mode of orientation is also evident from the analysis of orientation time constants [32]. Both the midpoint $E_0$ and the width $E_m$ of the transition obtained from the dichroism and the rotation times are closely related to each other.

The electrochemical data obtained from dichroism experiments contain a wealth of information about the ion atmosphere of nucleic acid helices. However, the interpretation of this information on the molecular level is quite involved. At present, we can only give a model which predicts the correct magnitude for the polarizability of short helix fragments. Many observations, e.g., the dependence of the polarizability upon the square of the helix length, remain unexplained.

The most important information concerning the nucleic acid structure comes from the limit reduced dichroism. The values observed for long helices with more than 1000 base-pairs are very close to that expected for the B-form of DNA. This observation indicates that the B-form (or a very similar form) with a packing of the base planes almost perpendicular to the long axis of the helix actually exists in dilute aqueous solution. However, this conclusion seems to be in contradiction to the relatively low values of the limit dichroism observed for the short fragments. Our results for the short fragments might be explained by a propellor-like twist of the base-pairs [14]. A propellor twist was recently detected also by X-ray

crystallography of a self-complementary dodecamer helix [33,34]. However, if the propellor twist is present to a large extent in all helices, it would be difficult to explain the high dichroism found for the long helices. It might be argued that the orientation curves for the long helices are distorted due to a statistical distribution of helix lengths and that this leads to artificially high extrapolations for the limit reduced dichroism. However, the high values found for long helices cannot be merely due to problems in the extrapolation, since the values measured are clearly higher for the long helices.

The observed dichroism and its chain length dependence may be explained by a bent structure of DNA [35]. Bending will result in reduced values of the dichroism. It may be expected that bending will lead to particularly low values of the dichroism at high chain lengths. However, it is known that electric fields induce an elongation of polymer chains. The elongation tendency is expected to increase with increasing chain length (elongation and especially its reverse process is also reflected in the dynamics of the orientation [32]). Thus, at high chain lengths the electric field will straighten bent helix structures resulting in high values of the reduced dichroism. Bending of a DNA helix was recently also found by X-ray crystallography for a self-complementary dodecamer [33,34].

In addition to the chain length dependence, the limit dichroism shows a clear dependence upon base sequence. The variation in the limit dichroism observed for fragments of very similar chain length is much higher than variations expected from the experimental uncertainty: the dichroism of the 76-base-pair fragment is $-1.11 \pm 0.03$, while the dichroism of a smaller (69-base-pair) and a larger (84-base-pair) fragment is $-1.27 \pm 0.03$ and $-1.21 \pm 0.02$, respectively. We do not find any correlation of the limit dichroism with simple parameters of the helix fragments like GC content. Thus, this is further evidence for the existence of variations in the secondary structure of the double helix resulting from more subtle differences in base sequence [36]. For example, it is possible that certain base sequences favour bending of the DNA helix.

Obviously bending of DNA helices has an influence on field-induced orientation, which should be considered directly in the orientation function. However, direct consideration of bending and its field dependence will lead to a rather complex orientation function. Since the bending effect has not yet been included in the orientation function, values obtained for the limit dichroism by conventional extrapolation procedures should be interpreted with caution. Nevertheless, the values for the limit dichroism are very useful for a comparison of various fragments. For example, our conclusions on the structure of DNA discussed above should be valid although bending has not been considered directly in our orientation function.

The results of independent investigations of DNA restriction fragments were recently published by Stellwagen [37] and also by Elias and Eden [38]. Since in both cases orientation was analyzed by birefringence measurements, whereas our data were obtained by measurements of the electrodichroism, the results and conclusions are complementary. The results should be identical with respect to the polarizability. The increase in the polarizability with the square of the chain length found in the present investigation corresponds to that published by Stellwagen, whereas Elias and Eden found an initial increase with the cube of the chain length. The other electric parameters obtained from the present analysis such as saturation field strength and saturation field range have not been determined previously. These parameters describing the polarization of the ion atmosphere can be obtained both by dichroism and birefringence measurements. An advantage in the case of dichroism measurements is the fact that the dichroism provides more detailed information about the structure.

## Acknowledgements

We want to thank R. Luce for performing some gel electrophoresis experiments and Dr. M. Teubner for helpful discussion. The technical assistance of R. Weise is gratefully acknowledged. This work was supported by grants of the NIH (CA20279) and the NSF (PCM77-15033).

## References


1 E. Fredericq and C. Houssier, Electric dichroism and electric birefringence (Clarendon Press, Clarendon, TX, 1973).
2 C.T. O'Konski, Molecular electrooptics (Marcel Dekker, part 1, 1976 and part 2, 1978).
3 W. Hillen, R.D. Klein and R.D. Wells, Biochemistry 20 (1981) 3748.
4 S.C. Hardies, R. Patient, R.D. Klein, F. Ho, W.S. Reznikoff and R. Wells, J. Biol. Chem. 254 (1979) 5527.
5 S.C. Hardies, W. Hillen, T.C. Goodman and R.D. Wells, J. Biol. Chem. 254 (1979) 10128.
6 V. Hershfield, H. Boyer, L. Chow and D. Hilinski, J. Bacteriol. 126 (1976) 447.
7 R.D. Wells, S.C. Hardies, G.T. Horn, B. Klein, J.E. Larson, S.K. Neuendorf, N. Panayotatos, R.K. Patient and E. Selsing, Methods Enzymol. 65 (1980) 327.
8 A. Oka, N. Nomura, M. Morita, H. Sugisaki, K. Sugimoto and M. Takanami, Mol. Gen. Genet. 172 (1979) 151.
9 H. Ohmori and J. Tomizawa, Mol. Gen. Genet. 176 (1979) 161.
10 J. Tomizawa, personal communication.
11 A.M. Maxam and W. Gilbert, Proc. Natl. Acad. Sci. U.S.A. 74 (1977) 560.
12 R.A. Jorgensen and W.S. Reznikoff, J. Bacteriol. 138 (1979) 705.
13 J.G. Sutcliffe, Nucleic Acid Res. 5 (1978) 2721.
14 H. Grunhagen, Thesis, University of Braunschweig (1974).
15 D. Porschke, Nucleic Acid Res. 8 (1980) 1591.
16 J. Nelder and R. Mead, Comput. J. 7 (1964/65) 308.
17 D. Ding, R. Rill and K.E. Van Holde, Biopolymers 11 (1972) 2109.
18 X. Emonds-Alt, C. Houssier and E. Fredericq, Biophys. Chem. 10 (1979) 27.
19 S. Sokerov and G. Weill, Biophys. Chem. 10 (1979) 161.
20 M. Hogan, N. Dattagupta and D.M. Crothers, Proc. Natl. Acad. Sci. U.S.A. 75 (1978) 195.
21 C. Marion and B. Roux, Biochem. Biophys. Res. Commun. 95 (1980) 27.
22 C.T. O'Konski, K. Yoshioka and W. Orttung, J. Phys. Chem. 63 (1959) 1558.
23 M. Mandel, Mol. Phys. 4 (1961) 489.
24 K. Kikuchi and K. Yoshioka, Biopolymers 15 (1976) 583.
25 E. Neumann and A. Katchalsky, Proc. Natl. Acad. Sci. U.S.A. 69 (1972) 993.
26 J.P. McTague and J.H. Gibbs, J. Chem. Phys. 44 (1966) 4295.
27 F. Oosawa, Biopolymers 9 (1970) 677.
28 C. Hornick and G. Weill, Biopolymers 10 (1971) 2345.
29 G.S. Manning, Biophys. Chem. 9 (1978) 65; (a) E. Charney, K. Yamaoka and G.S. Manning, Biophys. Chem. 11 (1980) 167.
30 M. Eigen and G. Schwarz, J. Colloid Interface Sci. 12 (1957) 181.
31 M. Fixman, Macromolecules 13 (1980) 711.
32 S. Diekmann, W. Hillen, B. Morgeneyer, R.D. Wells and D. Porschke, Biophys. Chem., in the press.
33 R.M. Wing, H.R. Drew, T. Takano, C. Broka, S. Takana, K. Itakura and R.E. Dickerson, Nature 287 (1980) 755.
34 H.R. Drew, R.M. Wing, T. Takano, C. Broka, S. Tanaka, K. Itakura and R.E. Dickerson, Proc. Natl. Acad. Sci. U.S.A. 78 (1981) 2179.
35 E. Selsing, R.D. Welss, C.J. Alden and S. Arnott, J. Biol. Chem. 254 (1979) 5417.
36 R.D. Wells, T.C. Goodman, W. Hillen, G.T. Horn, R.D. Klein, J.E. Larson, U.R. Muller, S.K. Neuendorf, N. Panayotatos and S.M. Stirdivant, Progr. Nucleic Acid Res. Mol. Biol. 24 (1980) 167.
37 N.C. Stellwagen, Biopolymers 20 (1981) 399.
38 J.G. Elias and D. Eden, Macromolecules 14 (1981) 410.